Biochemical and Biophysical Research Communications **260,** 597–599 (1999)
Article ID bbrc.1999.0885, available online at http://www.idealibrary.com on IDEAL®

Rotation of *Escherichia coli* F_1-ATPase

Hiroyuki Noji,* Katrin Häsler,† Wolfgang Junge,† Kazuhiko Kinosita, Jr.,*,‡ Masasuke Yoshida,*,§,[1] and Siegfried Engelbrecht†

**CREST team13 (Core Research for Evolutional Science and Technology) "Genetic Programming" Team 13, Teikyo University Biotechnology Research Center 3F, Nogawa 907, Miyamae-ku, Kawasaki 216-0001, Japan; †Abteilung Biophysik, Fachbereich Biologie/Chemie, Universität Osnabrück, D-49069, Germany; ‡Faculty of Science and Technology, Keio University, Yokohama 223-8522, Japan; and §Research Laboratory of Resources Utilization, Tokyo Institute of Technology, Yokohama 226-8503, Japan*

Received May 21, 1999

By applying the same method used for F_1-ATPase (TF_1) from thermophilic *Bacillus* PS3 (Noji, H., Yasuda, R., Yoshida, M., and Kinosita, K., Jr. (1997) *Nature* 386, 299–302), we observed ATP-driven rotation of a fluorescent actin filament attached to the γ subunit in *Escherichia coli* F_1-ATPase. The torque value and the direction of the rotation were the same as those observed for TF_1. F_1-ATPases seem to share common properties of rotation irrespective of the sources.

Driven by a downhill flow of protons, F_oF_1-ATPase synthesizes ATP (1). It can also catalyze the reverse reaction, hydrolysis of ATP pumping protons in the opposite direction. ATP synthesis and hydrolysis occur at the membrane-protruding portion, F_1 with a subunit composition of $\alpha_3\beta_3\gamma\delta\epsilon$. Isolated F_1-ATPase exhibits strong ATP hydrolysis activity, hence called F_1-ATPase, and its $\alpha_3\beta_3\gamma$ subcomplex is the minimum stable ATPase-active unit (2). F_o, the membrane-embedded portion, mediates the proton-translocation through the membrane. The γ subunit of F_1-ATPase is a major component of the "shaft" connecting F_1 to F_o and is responsible for the exchange of energy between the two portions (3). Boyer proposed a rotational movement of γ subunit within F_1-ATPase during the coupling reaction (4). This rotational model gained strong support from a crystal structure of F_1-ATPase in which the central γ subunit is surrounded by an $\alpha_3\beta_3$ cylinder (5). Biochemical and spectroscopic studies (6–8) suggested a rotation which was then proven by its direct observation in a single $\alpha_3\beta_3\gamma$ subcomplex of F_1-ATPase from thermophilic *Bacillus* PS3 (TF_1) (9). Attachment of a fluorescent actin filament to the γ subunit enabled us to observe its counterclockwise rotation (as viewed from F_o side) under an inverted fluorescence microscope. The analysis of the rotation at low ATP concentrations revealed that this enzyme is a highly efficient stepping-motor with discrete 120-degree rotation driven by each ATP hydrolysis (10). To confirm that these properties of the rotation are common features irrespective of the source of the enzyme, we applied the same experimental approach to F_1-ATPase (EF_1) from *Escherichia coli.*

MATERIALS AND METHODS

Strain and plasmids. EF_1 containing 6 additional His residues (His-tag) at the N-termini of the three β subunits and a γK107C mutation (corresponding to γS107C of TF_1) for the rotation assay was obtained by expression of the plasmid pKH7 in *E. coli* strain DK8. pKH7 was constructed from plasmids pACWU1.2 (βflag-tag/Cys-less) (11) and pSK7 (βHis-tag) (12). γK109 in pACWU1.2 was substituted with Cys by PCR using oligonucleotide primers, 5′-CCG ACT GCG GCG TTC AAG CCG ACC TCG C-3′ and 5′-GAA CGC CGC AGT CGG TCC AGG TCT TC-3′ to yield pKH3 (βflag-tag/γK109C). βC137 in pSK7 was substituted with Ala by PCR using oligonucleotide primers, 5′-CCT GATGGC TCC GTT CGC TAA GGG CGG-3′ and 5′-GAA CGG AGC CAT CAG GTC GAT AAC TTT G-3′, and its PmeI-SacI fragment coding for the N-terminal region of β (His-tag/C137S) was subcloned into pACWU1.2 to yield pKH4 (βHis-tag/Cys-less). The KpnI-PmeI fragment coding γK109C of pKH3 was subcloned into pKH4 to yield pKH7 (βHis-tag/γK109C). In all cases, correct mutations were confirmed by DNA sequencing.

Protein preparations. E. coli strain DK8 was transformed with pKH7. Cells were collected at $O.D._{595}$ = 0.8. Membranes were purified as described by Wise (13). EF_1 was extracted by EDTA treatment and applied to an anion-exchange column (Tosoh Fractogel TSK-DEAE 650(S), Toyo Soda, Japan) equilibrated with buffer A (50 mM Tris-SO_4, 2 mM EDTA, 10% (v/v) methanol, pH 7.8). EF_1 was eluted stepwise with 75 mM, 150 mM, and 500 mM Na_2SO_4 in buffer A. The 75–150 mM Na_2SO_4 fraction containing EF_1 was diluted 4-fold with buffer A and applied to Ni-NTA agarose (Qiagen). Pure EF_1 was eluted with 100 mM imidazole in buffer A. The yield of purified EF_1 was around 10 mg starting from a 8-liter culture. The purified EF_1

[1] To whom correspondence should be addressed at Research Laboratory of Resources Utilization, Tokyo Institute of Technology, Yokohama 226-8503, Japan. Fax: 81-45-924-5277. E-mail: myoshida@res.titech.ac.jp.

0006-291X/99 $30.00

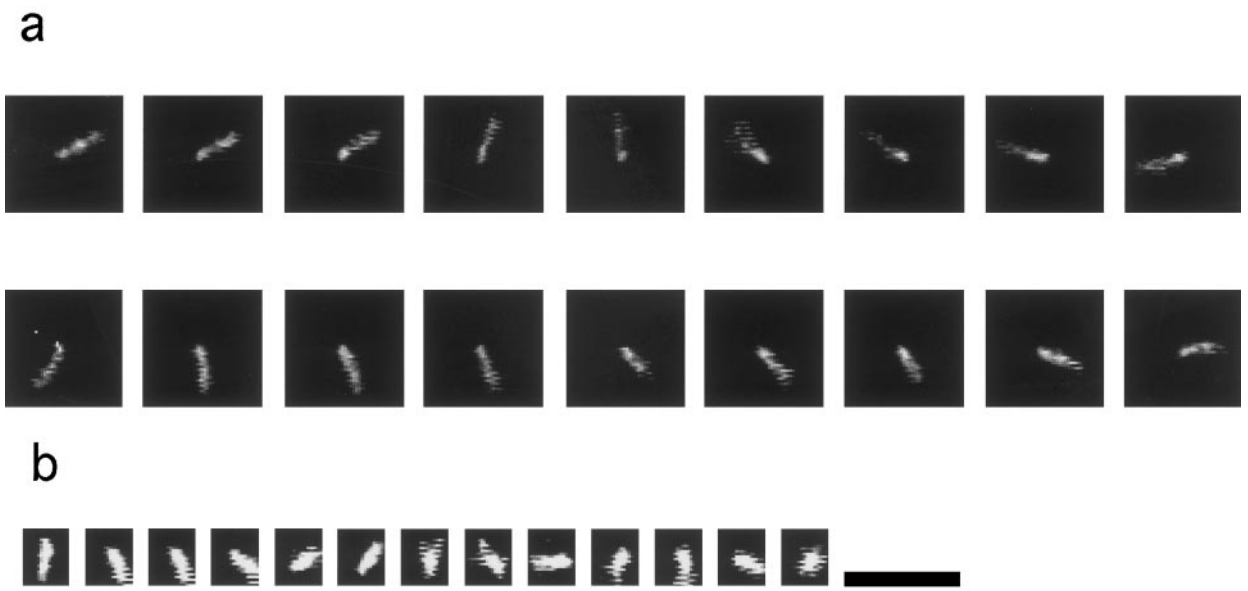

FIG. 1. Sequential images of a rotating actin filament attached to the γ subunit in EF_1 at 2 mM ATP. (a) A rotating filament with the axis at one end. The filament length, 2.2 μm; rotational rate, 0.77 rps.; time interval between images, 66 ms. (b) A rotating filament with the axis close to the middle of the filament. One length from the axis to tip, 1.2 μm, another length, 0.7 μm; rotational rate, 3.1 rps; time interval between images, 33 ms. Scale bar, 5 μm in a and b.

was biotinylated at the sole Cys, γK109C and conjugated with streptavidin. Rabbit skeletal actin filaments were biotinylated and stained with phalloidin-tetramethylrhodamine B (9).

Rotation assay. Proteins were infused into a flow chamber constructed with two coverslips (10). A solution (0.5% 2-mercaptoethanol, 0.2 mg/ml glucose oxidase, 30 U/ml catalase, 33 mM glucose, 2 mM $MgCl_2$, and 2 mM MgATP) was infused into the flow chamber and observed on an inverted fluorescent microscope (IX70, Olympus, Japan) at 22°C. Images were recorded with an intensified CCD camera (ICCD-350F, Video Scope, USA) on an 8 mm video tape. Rotating filaments with the axis at one end were selected, and the rotation angle was calculated from the centroid of the filament image with an analyzing software, NIH image.

RESULTS AND DISCUSSION

Using a mutant EF_1 in which all Cys residues had been substituted by Ala (11), we introduced further mutations similar to the mutant TF_1 used previously (9), as follows. At the N-termini of β subunit, His-tags were added to immobilize EF_1 on Ni-NTA-coated coverslips. The γK109C mutation was introduced and the single Cys residue was biotinylated for the attachment of the actin filament through streptavidin. SDS–PAGE analysis indicated that our preparation of EF_1 had lost most of the δ subunit and the amount of the ϵ subunit was also substoichiometric (data not shown). Upon applying EF_1 to the rotation assay, the enzyme concentration would be less than nM, thus causing furhter loss of ϵ due to the nM range K_d (14). The observed rotational properties would be, therefore, mainly derived from the $\alpha_3\beta_3\gamma$ subcomplex of EF_1.

EF_1 was infused into the flow chamber after conjugation with streptavidin. Then, we infused the actin filament into the flow chamber to attach it to the streptavidin-conjugated EF_1 immobilized on the surface of the coverslip and observed with the fluorescent microscope. In the presence of ATP, some of the actin filaments rotated continuously with the axis at one end of the filament (Fig. 1a). Rotating filaments with the axis near the middle were also observed (Fig. 1b). The direction of rotation was counterclockwise without exception, the same direction as observed for TF_1. The

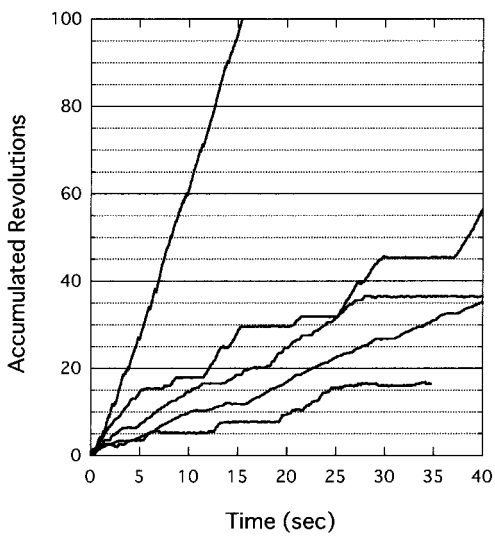

FIG. 2. Time-course of the rotation of the γ subunit. Images of the rotating actin filaments were recorded with the intensified CCD camera, and the centroids were analyzed. Each line represents the anti-clockwise rotation of one filament.

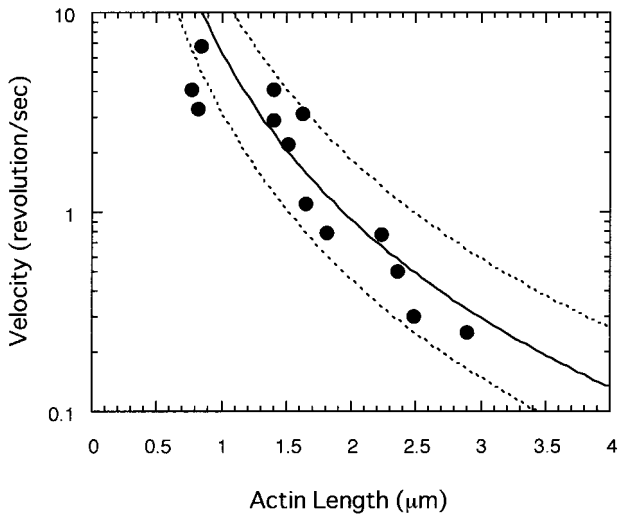

FIG. 3. Rotational rate in revolutions per second (rps) versus the length of the actin filament. Filaments that rotated around one end for >5 revolutions without an unnatural intermission were analyzed. Lines show the rotational rate under a constant torque of 40 pNnm (solid line), 80 pNnm (upper dashed line) and 20 pNnm (lower dashed line).

time-courses of the rotation of individual actin filaments are shown in Fig. 2. The filaments rotated continuously for several minutes and the rotational rate was up to 6.7 revolutions/sec. As hydrolysis of one ATP is assumed to drive a 120-degree rotation (10), 83 revolutions/sec were expected from the ATPase activity (42 μmole/min/mg; 250 turn-over/sec) of the free (not immobilized) EF_1 in solution determined by Pi measurement. The reason for the slow rate of observed rotation might be the hydrodynamic friction against rotating actin filament that would limit the rotational velocity of the γ subunit (10). Longer actin filaments rotated slower (Fig. 3). Nevertheless, the rotational torque values calculated from the rotational rate and length of individual actin filaments were constantly at around 40pNnm. This value well agrees with the value obtained for the rotation of TF_1 (10).

Now F_1-ATPases from two sources, *E. coli* and thermophilic *Bacillus* PS3, have shown rotation. They are powerful motors, which exert torques of 40 pNnm irrespective of the load. Rotation assay of EF_1 will be useful due to the wealth of genetic and physiological studies on EF_1. The rotation assay will be applied to mitochondrial and chloroplast F_1-ATPases in the near future. It will reveal common properties of rotational coupling of F_oF_1-ATPases as well as specific functions for each enzyme from different sources.

ACKNOWLEDGMENTS

We thank Dr. Robert K. Nakamoto and Dr. Holger Lill for the expression vectors, pACWU1.2 and pBSK; Dr. Ryohei Yasuda for the programming of the image analysis; and Dr. Toru Hisabori and Dr. Eiro Muneyuki for critically reading the manuscript. This work was supported in parts by CREST (Core Research for Evolutional Science and Technology) to K.K. and M.Y., and Human Frontier Science Program to W.J. and M.Y.

REFERENCES

1. Junge, W., Lill, H., and Engelbrecht. S. (1997) *Trends. Biochem. Sci.* **22,** 420–423.
2. Matsui, T., and Yoshida, M. (1995) *Biochim. Biophys. Acta* **1231,** 139–146.
3. Lucken, U., Gogol, E. P., and Capaldi, R. A. (1990) *Biochemistry* **29,** 5339–5343.
4. Boyer, P. D. (1993) *Biochim. Biophys. Acta* **1140,** 215–250.
5. Abrahams, J. P., Leslie, A. G. W., Lutter, R., and Walker, J. E. (1994) *Nature* **370,** 621–628.
6. Duncan, T. M., Bulyin, V. V., Zhou, Y., Hutcheon, M. L., and Cross, R. L. (1995) *Proc. Natl. Acad. Sci. USA* **92,** 10964–10968.
7. Aggeler, B., Ogilvie, I., and Capaldi, R. A. (1997) *J. Biol. Chem.* **272,** 19621–19624.
8. Sabbert, D., Engelbrecht, S., and Junge, W. (1996) *Nature* **381,** 623–625.
9. Noji, H., Yasuda, R., Yoshida, M., and Kinosita, K., Jr. (1997) *Nature* **386,** 299–302.
10. Yasuda, R., Noji, H., Kinosita, K., Jr., and Yoshida, M. (1998) *Cell* **93,** 1117–1124.
11. Phillip, H. K., Ketchum, C. J., and Nakamoto, R. K. (1998) *FEBS Lett.* **426,** 217–220.
12. Kirberich, S., Stolte, C., and Lill, H. (1998) *Biochim. Biophys. Acta, EBEC short reports* **10,** 50.
13. Wise, J. G. (1990) *J. Biol. Chem.* **265,** 10403–10409.
14. Kato, Y., Sasayama, T., Muneyuki, E., and Yoshida, M. (1995) *Biochim. Biophys. Acta* **1231,** 275–281.